International Journal of Computational and Theoretical Chemistry
2022; 10(2): 14-20
http://www.sciencepublishinggroup.com/j/ijctc
doi: 10.11648/j.ijctc.20221002.11
ISSN: 2376-7286 (Print); ISSN: 2376-7308 (Online)

Theoretical Study on the Stereo Electronic Interactions of Busulfan Anti-cancer Drug with Modified Nano Cellulose Surface

Mohammad Rizehbandi[1], Maryam Ariannezhad[2, *]

[1]Chemistry Department, Faculty of Science, Guilan University, Guilan, Iran

[2]Chemistry Department, Comprehensive University of Applied Sciences, Dr. Abidi Hygienic Company, Tehran, Iran

Email address:
mariam.ariannezhad@gmail.com (Maryam Ariannezhad)

[*]Corresponding author

To cite this article:
Mohammad Rizehbandi, Maryam Ariannezhad. Theoretical Study on the Stereo Electronic Interactions of Busulfan Anti-cancer Drug with Modified Nano Cellulose Surface. *International Journal of Computational and Theoretical Chemistry*. Vol. 10, No. 2, 2022, pp. 14-20.
doi: 10.11648/j.ijctc.20221002.11

Received: July 13, 2022; **Accepted**: August 12, 2022; **Published**: August 24, 2022

Abstract: In this study, the interaction of Busulfan anticancer drug with PEG-modified cellulose was investigated. The impacts of the stereo electronic effect associated with donor-acceptor electron delocalizations, dipole-dipole interactions, and total steric exchange energies on the structural and electronic properties and reactivity of modified cellulose in interaction with Busulfan anticancer drug was studied based on the Density Functional Theory (DFT) calculations by using B3LYP/(6-31G, 6-31G*) level of theory in the gas phase, and water solution. Thermodynamic functional analysis indicates that the relative energies (ΔE), free Gibbs energies (ΔG) and enthalpies (ΔH) are negative for of Busulfan anticancer drug-PEG-modified cellulose system, but the calculated entropies (ΔS) are Positive, suggesting thermodynamic favorability for covalent attachment of dye on PEG-modified cellulose and these results confirm the structural stability of the Busulfan in gas phases. Delocalization of charge density between the bonding or lone pair and antibonding orbitals calculated by NBO (natural bond orbital) analysis. The calculated LUMO-HOMO energy bond gap shows that charge density transfer occurs within the molecules and the semi-conductivity of PEG could be justified. Also, based on the parameters obtained for the Busulfan drug in the absence of cellulose, it can be said that due to the presence of cellulose, the interaction between the electronegative oxygen atom of cellulose and the carbons of Busulfan has the least electron coverage and is more affected by the external magnetic field, so They have the lowest σiso and the highest δ or chemical shift, but in the absence of cellulose, carbon does not interact with oxygen, it has the highest electron coverage and appears in the ^{13}CNMR spectrum at a lower δ chemical shift.

Keywords: Cellulose, PEG, Thermodynamic Functional, Delocalization

1. Introduction

The fast increase in population causes, the more energy demand people require. Standard quality of food, drugs, and health parameters are changing and among them health parameters are highly interlinked to the industry of pharmaceutical compounds since they need to be upgraded as the population increases [1-3] In recent decades, enormous concentrated research on enhancement of produced drugs such as quality of dosage form via particle size reduction has been applied. Quality guarantee and biocompatibility of medicine are the majority of concerns challenging the pharmaceutical industry. For instance, the conventional methods for micronizing particle size of drugs, including crushing, grinding, hammering, milling, etc. [4-7] Suffer from some difficulties like consuming high energy or unfinished toxic solvents in the obtained products, which make those methods ineffective. Working on drug delivery systems and nanocarriers are the significant type of methods to transport API (active pharmaceutical ingredients) to progress the quality of remedial effect [8-12]. Recently, software-based modeling has been used in pharmaceutical manufacturing areas due to its preferable behavior and accuracy in the prognosis of biochemical processes. These models can be

performed for the production of either small molecules or biopharmaceuticals containing intricate processes [13-16].

There are numerous drug therapies in the field of oncology that increase the risk of single or multiple drug interactions (DDIs), which often lead to detrimental toxicity and unpredictable treatment outcomes [17]. HSCT patients receive an average of at least eight or more medications during their remedy process and expose to complex drug regimens consisting of various sorts of drugs for long time, which interact with each other. The liver is one of the vital and vulnerable organs in the body that plays a prominent and essential role in the detoxification of xenobiotics, environmental pollutants, and chemical drugs since all the substances we enter our body pass through the liver [18] Acute liver failure is caused by a number of factors, including viral hepatitis, toxic liver damage from toxins and drugs, and ischemia. Chemicals and drugs, especially chemotherapy drugs, have devastating effects on the liver and the destructive effects that chemotherapy drugs have on the liver have no obvious symptoms. Of course, in some people, these side effects can sometimes include fatigue, jaundice, nausea, weight loss, and abdominal pain. Research has shown that many people develop multiple liver problems after being treated for cancer. Complications were calculated by taking liver enzyme in the blood. The treatment methods were different, and methods such as radiation therapy, chemotherapy and bone marrow transplantation were used to treat the patients under study. The result was that 1% to 53% of the recovered patients had liver problems [19, 20]. Meanwhile, radiation therapy greatly increased the risk of liver disease. Also, other factors such as Busulfan, thioguanine, or even liver surgery affect liver vulnerability. Furthermore, Survivors of hepatitis metabolic syndrome are no exception. Many studies to evaluate the protective effects of various chemical compounds in order to reduce the effects of toxic drugs such as cisplatin has been done, but unfortunately, some of the compounds used as protective agents to reduce the adverse effects of Busulfan in therapies reduce the anticancer effects, while others do not completely eliminate the effects of the drug [21]. The alkylating anti-cancer agent Busulfan (1,4-butanedioldimethyl- sulfonate) at high doses is extensively used in lymph node, hematological and immune system malignancies cancers [22]. In fact, this agent, by alkylating process, slows down the growth of cancer cells or even stops them through alkylating the DNA and according to a chain process, this growth and development is reduced after a while or stops [23]. When two important groups of methane and sulfonate in the Busulfan agent release, it obtains the ability of alkylating. On the other hand, this agent in the cell nucleus via a difficult interaction with the DNA molecule, and in the cystocele by alkylating the sulfhydryl group of the molecule glutathione and cysteine, reduces the growth and development and finally stops, which leads to death of cell. The side effects of Busulfan have been observed in important parts of the body, including the liver and scalp; For example, hepatotoxicity and metabolic disorders in liver cells, hair, eyebrow, and eyelash loss. Also, using high doses of this drug leads to destroying marrow cells [24, 25]. For this reason, efforts have been made to combine it with other drugs, like other anti-cancer drugs, to prevent side effects. Many compounds using nanotechnology knowledge have been applied as drug carriers, but one of the most important materials in this field are modified nano celluloses. The advantages of this compound include biodegradability, high compatibility, hydrophilicity, recyclability and non-toxicity, and the significant features of this compound in terms of application can be a large special surface area, cost-effective, low weight, etc. [26, 27]. Cellulose is found in abundance in nature, but although existence of hydrophilic functional groups, there are hydrocarbon rings that lead to low solubility in water and cannot be used as a drug carrier. Therefore, these nano celluloses are modified by the processes of bonding, acetylation, or even oxidation. Important reactions of these nano celluloses include the formation of ionic groups (carboxymethylation, oxidation, sulfonation) and other reactions. Busulfan has a sulfonate functional group, it is likely that oxidation reactions and subsequent sulfonation will be used as an interaction between Busulfan and modified nano celluloses [28]. In this study, we investigate the interaction of Busulfan anticancer drug with PEG-modified cellulose based on the Density Functional Theory (DFT) calculations via B3LYP/(6-31G, 6-31G*) level of theory in the gas phase and water solution.

2. Mechanism of Busulfan

Busulfan as an alkylating agent, contains two unstable methanesulfonate groups, which there are in opposite end parts of a four-carbon alkyl chain. Hydrolysis of Busulfan leads to releasing methane sulfonate groups and producing positive carbonium ions. Therefore, DNA is alkylated by these carbonium ions, which affects the interposition of DNA replication and RNA transcription and finally, causing to the disconnection of nucleic acid function. Particularly this mechanism generates guanine-adenine interesting crosslinks, which form through a SN2 reaction by attacking guanine N7 as a nucleophile on adjacent carbon and metylate discloses as a leaving group. This type of detriment cannot be recovered by cellular machinery and, so the cell undertakes apoptosis.

Moreover, Busulfan reacts spontaneously with the sulfhydryl groups of the endogenous tripeptide GSH or through GST enzymes Thereby, disconnection of the cellular redox equilibrium, which leads to oxidative stress. Also, forming of methane sulfonic acid as a known metabolite of Bu is the result of Bu with GSH and Bu hydrolysis. Methanesulfonic acid was characterized in the blood, and almost completely removed from the blood during 10–15 minutes, and was detected in large quantities in the urine within 24 hours [29, 30].

3. Optimal Structure of Busulfan

The structural parameters calculated using the theoretical level calculations B3LYP / 6-31G * for Busulfan compounds in the presence of cellulose as modified structure are shown in (Table 1) and Busulfan in the absence of cellulose (Table 2). The comparison of changes in structural parameters in

Busulfan and cellulose used alone with the presence of these two compounds indicates that the change in structural parameters in the involved areas is considerable. Based on the results of the obtained calculations, there is a direct relationship between changes in structural parameters and the amount of resonant energies due to the lack of electron localization. In fact, the higher the resonance energy due to electron transfer in a bond, the greater the change in the structural parameters of that bond. Evaluation of changes in structural parameters, including bond lengths, bond angles, and two-dimensional angles in a mixture of pegylated procarbazine cellulose, shows that the length of the bonds and the two- dimensional and angles of the involved atoms change, which can be a way to convince the electron interactions between Busulfan and cellulose, while in the absence of cellulose, carbon does not interact with oxygen, it has the highest electron coverage and appears in the ^{13}CNMR spectrum at a lower δ chemical shift. Therefore, the difference in structural parameters in the complex of Busulfan-cellulose drug with reactive raw materials can be increased by increasing the resonant energies due to electron instability by the molecule of Busulfan to cellulose and also by the cellulose used in molecule procarbazine. Therefore, changes in structural parameters can be one of the ways to convince the physical adsorption reaction through transferring electron through two involved systems in the reaction. s. The geometry of compound was initially optimized using the B3LYP/3-21G model and reoptimized using the B3LYP/6-31G model and B3LYP/6-311+G* model demonstrating that the corresponding geometries in Figure 2.

Table 1. *NMR parameters for all atoms of Busulfan in the presence of cellulose.*

Atoms	Isotropic	anisotropy	σ_{11}	σ_{22}	σ_{33}	σ_{11}-σ iso	σ_{33}-σ iso	Δσ	δ	η	Ω	κ
1 O	285.4784	41.1221	285.1043	305.0079	296.323	-10.3741	0.8446	1.2669	-10.3741	-0.83717	11.2187	2.54829
2 O	229.6921	43.639	253.99	257.4684	207.6179	14.2979	-32.074	-48.1113	-32.0742	-0.10845	-46.3721	-1.15002
3 C	114.4934	45.1266	138.4647	103.0572	101.9582	23.9713	-12.535	-18.8028	23.9713	0.045846	-36.5065	0.939794
4 C	119.2442	36.6655	136.5113	109.7591	111.4623	17.2671	-7.7819	-11.6729	17.2671	-0.09864	-25.049	1.135985
5 C	102.6824	18.7732	115.1698	111.5389	111.3386	2.4874	-1.3438	-2.01575	2.4874	0.080526	-3.8312	0.895411
6 C	116.8305	25.483	116.0853	131.4056	103.0005	-0.7452	-13.83	-20.745	-13.83	-1.10776	-13.0848	-3.34169
7 C	84.5824	25.747	97.2338	88.0328	68.4806	12.6514	-16.102	-24.1527	-16.1018	0.571427	-28.7532	-0.36
8 O	248.1247	63.7925	246.8047	243.1161	254.4533	-1.32	6.3286	9.4929	6.3286	-0.58285	7.6486	-1.96452
9 C	116.0484	66.1904	102.552	128.8136	116.7797	-13.4964	0.7313	1.0969	-13.4964	-0.89164	14.2277	2.691623
10 O	294.081	35.3183	265.6098	311.5539	305.0793	-28.4712	10.9983	16.49745	-28.4712	-0.22741	39.4695	1.328081
11 O	295.0453	49.7667	324.2214	287.6674	273.2471	29.1761	-21.798	-32.6973	29.1761	0.49425	-50.9743	0.434213
12 O	296.495	64.0046	275.8546	313.6366	299.9937	-20.6404	3.4987	5.2481	-20.6404	-0.66098	24.1391	2.130353
13 H	30.4461	17.4978	34.9841	32.4119	23.9421	4.538	-6.504	-9.7559	-6.504	0.39548	-11.042	-0.53409
14 H	28.5543	3.9057	28.8487	28.3825	28.4317	0.2944	-0.1226	-0.1839	0.2944	-0.16712	-0.417	1.235971
15 H	28.9717	2.3917	30.3653	28.3405	28.2094	1.3936	-0.7623	-1.1435	1.3936	0.094073	-2.1559	0.878334
16 H	28.7569	4.247	29.1448	27.9743	29.1515	0.3879	0.3946	0.59195	0.3946	-2.96629	0.0067	-350.418
17 H	29.1641	4.4383	29.2336	30.4625	27.7962	0.0695	-1.3679	-2.05185	-1.3679	-0.89838	-1.4374	-2.70989
18 H	27.9732	4.7291	30.9361	27.5827	25.4007	2.9629	-2.5725	-3.8587	2.9629	0.736441	-5.5354	0.211638
19 S	302.4461	17.4978	34.9841	32.4119	23.9421	4.538	-6.504	-9.7559	-6.504	0.39548	-11.042	-0.53409
20 S	289.5543	3.9057	28.8487	28.3825	28.4317	0.2944	-0.1226	-0.1839	0.2944	-0.16712	-0.417	1.235971

Table 2. *NMR parameters for all atoms of Busulfan in the absence of cellulose.*

atoms	Isotropic	anisotropy	σ_{11}	σ_{22}	σ_{33}	σ_{11}-σ iso	σ_{33}-σ iso	Δσ	δ	η	Ω	κ
1 O	-32.8995	603.494	-162.905	-300.7918	367.9985	-131.0058	399.898	599.84705	399.898	-0.34480418	530.9038	-1.51944081
2 N	135.8646	99.6337	127.9717	124.3029	155.3193	-7.8929	19.4547	29.182	19.4547	-0.18858168	27.3476	-1.26830508
3 N	157.2465	100.485	218.4926	134.5643	118.6824	61.2461	-38.5641	-57.84605	61.2461	0.25931284	-99.8102	0.68175998
4 N	171.9513	93.5551	229.236	148.4929	138.1252	57.2847	-33.8261	-50.73925	57.2847	0.1809855	-91.1108	0.77241337
5 C	146.7137	29.0888	165.2822	126.9312	147.9278	18.5685	1.2141	1.8211	18.5685	-1.13076447	-17.3544	3.41973793
6 C	54.5446	178.187	-32.3815	48.3678	147.6475	-86.9261	93.1029	139.65435	93.1029	0.8673124	180.029	-0.10293008
7 C	61.8997	156.74	-18.9368	65.7545	138.8813	-80.8365	76.9816	115.47245	-80.8365	0.904626	157.8181	0.07327677
8 C	35.3963	100.826	-22.8773	28.2441	100.8223	-58.2736	65.426	98.1389	65.426	0.78136215	123.6996	-0.17345731
9 C	131.8717	38.8279	144.814	140.6485	110.1524	12.9423	-21.7193	-32.57885	-21.7193	0.19178795	-34.6616	-0.75964179
10 C	166.8687	32.2086	169.1556	149.986	181.4644	2.2869	14.5957	21.8936	14.5957	-1.31337312	12.3088	-4.11478779
11 C	167.7257	33.1991	163.4513	176.8919	162.834	-4.2744	-4.8917	-7.3376	-4.8917	-2.74763375	-0.6173	-44.5465738
12 C	67.3432	148.112	42.4646	20.8816	138.6833	-24.8786	71.3401	107.0102	71.3401	-0.30253672	96.2187	-1.44862485
13 C	67.932	165.659	32.7894	23.3143	147.6923	-35.1426	79.7603	119.64045	79.7603	-0.11879469	114.9029	-1.1649236
14 C	65.7564	173.789	29.8267	16.1934	151.249	-35.9297	85.4926	128.23895	85.4926	-0.1594676	121.4223	-1.22456089
15 C	72.2912	155.597	43.6083	28.8375	144.4279	-28.6829	72.1367	108.205	72.1367	-0.20476124	100.8196	-1.29301346
16 C	150.5095	53.0004	145.9298	173.7252	131.8736	-4.5797	-18.6359	-27.9539	-18.6359	-1.49149759	-14.0562	-4.95490246
17 H	27.8791	5.2164	27.5352	28.6635	27.4386	-0.3439	-0.4405	-0.66075	-0.4405	-2.56140749	-0.0966	-24.3602484
18 H	27.4021	9.2458	33.2189	28.83	20.1573	5.8168	-7.2448	-10.86715	-7.2448	0.60580002	-13.0616	-0.32796135
19 S	28.6619	7.0837	28.9606	32.666	24.3592	0.2987	-4.3027	-6.4541	-4.3027	-0.86118019	-4.6014	-2.61057504
20 S	27.9513	3.5253	27.8635	27.1859	28.8043	-0.0878	0.853	1.2796	0.853	-0.7943728	0.9408	-2.44068878

Drug loading on the polymer has a significant effect on the coverage parameters of the reacting atoms in the NMR spectrum. Spectra, ^{13}CNMR, ^{1}HNMR and for Busulfan, cellulose and drug-polymer complex are discussed in two ways based on the

amount of chemical shielding (σ) and chemical shifting (δ) (Table 1).

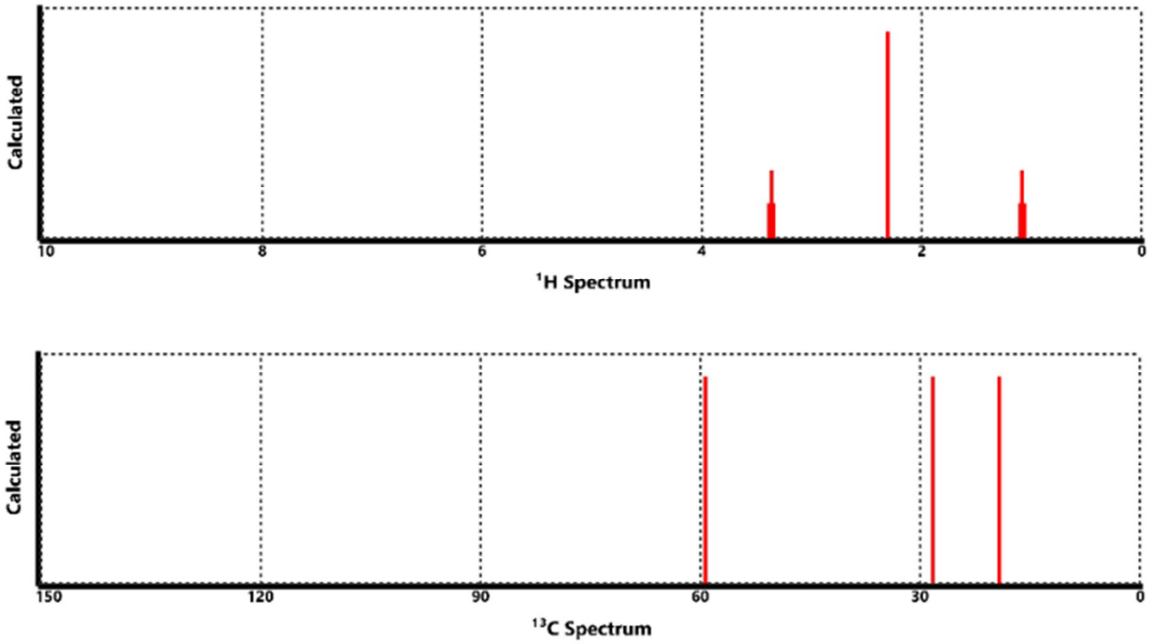

Figure 1. *NMR spectrum of carbon and hydrogen atoms of Busulfan in terms of chemical displacement (δ).*

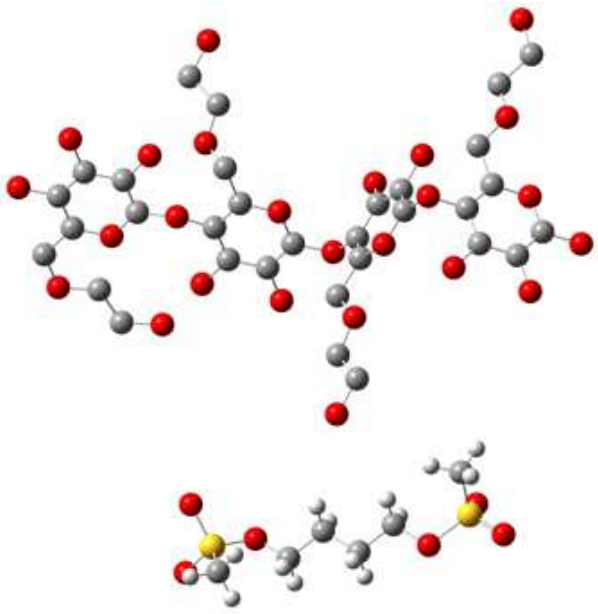

Figure 2. *Structure resulting from the reaction of Busulfan with cellulose.*

In the molecule of Busulfan, the isotropic parameter of chemical overlap or isotropic chemical coating (σiso) was investigated, where σiso, calculated for carbon atoms in the molecule, divides the nuclei into several groups in terms of the electrostatic environment they feel. On other words, the atoms of a molecule that are in different chemical areas have different chemical shift depending on the different chemical shielding. The effect of substitution (donor or acceptor) affects the chemical shift of the atoms in a molecule, and via changing the bond order from single (σ) to double (π) and vice versa, the amount of chemical overlap and shift of atoms is affected and They change. Based on the parameters obtained for Busulfan in the absence of cellulose, it can be said that carbon No. 8, which is attached to the electronegative atoms of oxygen No. 1 and nitrogen No. 2, has the lowest electron coverage and is more affected by the external magnetic field. They have the lowest σiso and the highest δ or chemical displacement. Carbon 11, on the other hand, has the highest electron shielding and appears at a lower δ chemical shift in the ^{13}CNMR spectrum (Figure 1).

In the presence of the drug, the isotropic parameter of chemical overlap or isotropic chemical coating (σiso) was investigated. The σiso, calculated for carbon atoms in the molecule, divides the nuclei into several groups in terms of the electrostatic environment they feel. Based on the parameters obtained from ^{13}CNMR calculations for Busulfan in the presence of cellulose, it can be said that carbon 123, which is attached to the electronegative oxygen atom, has the lowest electron coverage and is most affected by the external magnetic field, so the lowest σiso and the most It has a chemical displacement δ. Carbon 126, on the other hand, has the highest electron conductivity and appears at a lower δ chemical shift in the ^{13}CNMR spectrum. Also, based on the parameters obtained from ^{1}HNMR calculations for the drug in the presence of polymer, hydrogen 145 has the lowest electron coverage and is most affected by the external magnetic field, so it has the lowest σiso and the highest chemical shift (δ). Therefore, it can be said that isotropic chemical coverage (σiso) and maximum chemical displacement (δ) resulting from NMR calculations by GIAO method is a suitable parameter and scale to investigate the nature of drug-polymer interactions. According to the results obtained from the H-NMR spectrum based on chemical displacement in the spectrum of hydrogen theory number 90, it has the highest

chemical displacement (δ) of 4.4 ppm and the lowest chemical coverage (σiso) due to the presence of electronegative oxygen numbers 35 and 41 around the same hydrogen has appeared in the experimental spectrum at a chemical shift of 3.9 ppm and has the highest chemical shift (δ) and the lowest chemical overlap (σiso). Also, in the spectrum of hydrogen theory No. 112, it has the lowest chemical shift (-0.4 ppm) and the highest chemical saturation, and the same hydrogen appeared in the experimental spectrum in the chemical shift (-0.2 ppm) and has the lowest chemical shift (δ) and the highest chemical saturation (σiso). According to the obtained results from the C-NMR spectrum, pegylated cellulose based on the chemical shift in carbon theory spectrum No. 7 has the highest chemical shift (δ) 99.2 ppm and the lowest chemical shielding (σiso) due to the presence of electronegative oxygen 8 and 2. Around, the same carbon in the experimental spectrum has a chemical shift of 98 ppm and has the highest chemical shift (δ) and the lowest chemical overlap (σiso). Also, in the spectrum of carbon theory No. 49, it has the lowest chemical displacement (δ) of 51.8 ppm and the highest chemical saturation (σiso).

Figure 3 shows the energy gap of homo-LUMO molecular orbitals for the Busulfan-cellulose complex molecule. In the study of molecular orbital form of the drug, it can be observed that HOMO and LUMO orbitals are extended on half of the structure of Busulfan molecule. It is predicted that the possibility of reaction with electron-friendly species is in the part where the distribution of HOMO orbitals is higher and it is possible to react with nucleus species in the part where LUMO orbitals are more distributed. In the study of the molecular orbital form of the pegylated Busulfan-cellulose complex, it is observed that HOMO and LUMO orbitals are extended only on Busulfan molecule, and pegylated nanocellulose have a small share of LUMO molecular orbitals and have no rule in HOMO molecular orbital.

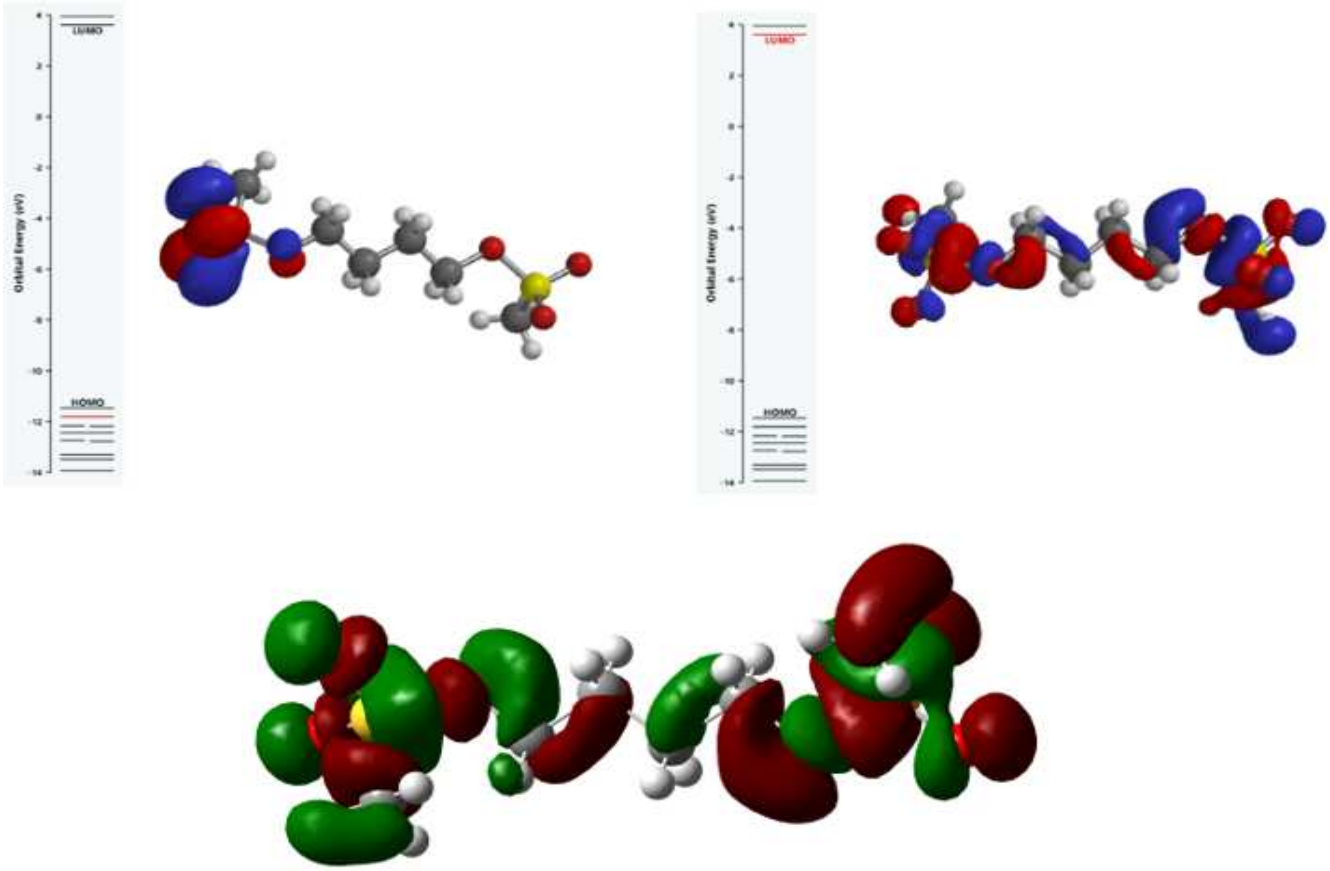

Figure 3. *Molecular orbital diagram for Busulfan molecule.*

4. Conclusion

Recently, density functional theory (DFT) has been used to analyze the characteristics of the inhibitor/ surface mechanism and to describe the structural nature of the inhibitor in the corrosion process. Furthermore, DFT is considered a very useful technique to probe the inhibitor/ surface interaction as well as to analyze the experimental data. Density functional theory (DFT). The inhibiting effect of these compounds can be attributed to their parallel adsorption at the metal surface. The parallel adsorption is attributed to the presence of one or more active centers for adsorption. In this work, we demonstrated the interaction of Busulfan anticancer drug with PEG-modified cellulose through the Density Functional Theory (DFT) calculations by using the B3LYP/(6-31G, 6-31G*) level of theory in the gas phase and water solution. The influences of the stereo electronic effect related to donor-acceptor electron delocalization, dipole-dipole interactions and total steric exchange energies on the

structural and electronic properties and reactivity of modified cellulose in interaction with Busulfan anticancer drug were investigated. Based on thermodynamic functional analysis relative energies (*ΔE*), free Gibbs energies (*ΔG*), and enthalpies (*ΔH*) are negative for of Busulfan anticancer drug-PEG-modified cellulose system, but the calculated entropies (*ΔS*) are Positive, indicating thermodynamic favorability for covalent attachment of dye on PEG-modified cellulose and these results verify the structural stability of the Busulfan in gas phases. Delocalization of charge density between the bonding or lone pair and antibonding orbitals calculated by NBO (natural bond orbital) analysis. These methods are used as a tool to determine the structural characterization PEG- modified cellulose during the adsorption reactions in the gas phase. In order to investigation of conductivity and electronic properties of in the reaction PEG-modified cellulose with Busulfan anticancer drug, the total electronic energy, dipole moment, orbital energies, charge density, density of state (DOS), LUMO-HOMO energy bond gaps, Adsorption energies (E_{Ad}), the global index includes hardness (η), electronegativity (χ), electrophilicity index (w), chemical softness (S) and electronic chemical potential (μ) were calculated. The calculated LUMO-HOMO energy bond gap shows that charge density transfer occurs within the molecules, and the semi-conductivity of PEG could be justified. Moreover, nuclear magnetic resonance (NMR) shielding tensors were calculated by using the Gauge Independent Atomic Orbital (GIAO) method in order to determination of intramolecular interactions and chemical properties of molecules. The IR, NMR, and UV spectrum were investigated.

References

[1] Reverchon, E. Adami, R. (2006). Nanomaterials and supercritical fluids. The Journal of supercritical fluids, 37 (1), 1-22.

[2] Vrána, A. Andrysek, T. (2001). The effect of particle size on bioavailability in cyclosporine preparations based on submicron dispersions. biomedical papers-palacky university in Olomouc, 145 (2), 9–15.

[3] Nishihata, T. Ishizaka, M. Yokohama, S. Martino, A. C. Gordon, R. E. (1993). Effects of Particle Size of Bulk Drug and food on the Bioavailability of U-78875 in Dogs. Drug development and industrial pharmacy, 19 (20), 2679–2698.

[4] Lashkarbolooki, M. Vaezian, A. Hezave, A. Z. Ayatollahi, S. Riazi, M. (2016). Experimental investigation of the influence of supercritical carbon dioxide and supercritical nitrogen injection on tertiary live-oil recovery. The Journal of Supercritical Fluids, 117, 260–269.

[5] Kalani, M. Yunus, R. (2011). Application of supercritical antisolvent method in drug encapsulation: a review. International journal of nanomedicine, 6, 1429-1442.

[6] Hezave, A. Z. Esmaeilzadeh, F. (2010). Crystallization of micro particles of sulindac using rapid expansion of supercritical solution. Journal of Crystal Growth, 12 (22), 3373-3383.

[7] Hezave, A. Z. Esmaeilzadeh, F. (2010). Micronization of drug particles via RESS process. The Journal of Supercritical Fluids, 52 (1), 84-98.

[8] Catchpole, O. J. Hochmann, S. Anderson, S. R. J. (1996). Gas anti-solvent fractionation of natural products. in Process Technology Proceedings, 1, 309–314.

[9] Dehghani, F. Foster, N. R. (2003). Dense gas anti-solvent processes for pharmaceutical formulation. Current Opinion in Solid State and Materials Science, 7 (4-5), 363-9.

[10] Imchalee, R. Charoenchaitrakool, M. (2015). Gas anti-solvent processing of a new sulfamethoxazole− l-malic acid cocrystal. Journal of Industrial and Engineering Chemistry, 25, 12–15.

[11] Foster, N. R. Kurniawansyah, F. Tandya, A. Delgado, C. Mammucari, R. (2017). Particle processing by dense gas antisolvent precipitation: ARISE scale-up. Chemical Engineering Journal, 308, 535–543.

[12] Kurniawansyah, F. Mammucari, R. Foster, N. R. (2017). Polymorphism of curcumin from dense gas antisolvent precipitation. Powder Technology, 305, 748–756.

[13] Xie, F. Gu, J. (2019). Computational methods and applications for quantitative systems pharmacology. Quantitative Biology, 7, 3–16.

[14] Jarada, T. N. Rokne, J. G. Alhajj, R. (2021). SNF–CVAE: computational method to predict drug–disease interactions using similarity network fusion and collective variational autoencoder. Knowledge-Based Systems, 212, 106585.

[15] Sliwoski, G. Kothiwale, S. Meiler, J. Lowe, E. W. (2014). Computational methods in drug discovery. Pharmacological reviews, 66 (1), 334–395.

[16] Jamal, S. B. Naz, S. Khan, R. Haider, A. Raza R. Z, Abbasi, S. W. (2020). Computational Methods in Road towards Drug Discovery against SARS-CoV2. Life and Science, 1, 6.

[17] Khandeparkar, A. Rataboli, P. V. (2017). A study of harmful drug–drug interactions due to polypharmacy in hospitalized patients in Goa Medical College. Perspectives in clinical research, 8 (4), 180.

[18] Neuman, M. G. (2020). Hepatotoxicity: mechanisms of liver injury. InLiver Diseases, 75-84.

[19] Koay E. J, Owen D, Das P. (2018). Radiation-induced liver disease and modern radiotherapy. InSeminars in radiation oncology, 28 (4), 321-331.

[20] Sharma, A. Houshyar, R. Bhosale, P. Choi, J. I. Gulati, R. Lall, C. (2014). Chemotherapy induced liver abnormalities: an imaging perspective. Clinical and molecular hepatology, 20 (3). 317-326.

[21] Dasari, S. Tchounwou, P. B. (2014). Cisplatin in cancer therapy: molecular mechanisms of action. European journal of pharmacology, 740, 364-378.

[22] Rodriguez-Galindo, C. Spunt, S. L. Pappo, A. S. (2003). Treatment of Ewing sarcoma family of tumors: current status and outlook for the future. Medical and pediatric oncology, 40 (5), 276–287.

[23] Lanvers-Kaminsky, C. Bremer, A. Dirksen, U. Jürgens, H. (2006). Cytotoxicity of treosulfan and busulfan on pediatric tumor cell lines. Anti-cancer drugs, 17 (6), 657–662.

[24] Iwamoto, T. Hiraku, Y. Oikawa, S. Mizutani, H. Kojima, M. Kawanishi, S. (2004). DNA intrastrand cross-link at the 5′-GA-3′ sequence formed by busulfan and its role in the cytotoxic effect. Cancer science, 95 (5), 454–458.

[25] Missailidis, S. (2008). Anticancer therapeutics. John Wiley & Sons.

[26] Karthick, T. Tandon, P. (2016). Computational approaches to find the active binding sites of biological targets against busulfan. Journal of molecular modeling, 22 (6), 1–9.

[27] McKenna, R. Neidle, S. Kuroda, R. Fox, B. W. (1989). Structures of three DNA cross-linking agents, ethane-1, 2-di (methylsulfonate), propane-1, 3-di (methylsulfonate) and n-butane-1, 4-di (methylsulfonate). Acta Crystallographica Section C: Crystal Structure Communications, 45 (2), 311–314.

[28] Garcia-Perez, L. van Roon, L. Schilham, M. W. Lankester, A. C. Pike-Overzet, K. Staal, F. J. (2021). Combining mobilizing agents with busulfan to reduce chemotherapy-based conditioning for hematopoietic stem cell transplantation. Cells, 10 (5), 1077.

[29] Chen, X. Liang, M. Wang, (2018). Progress on the study of the mechanism of busulfan cytotoxicity. Cytotechnology, 70 (2), 497–502.

[30] Hao, C. Ma, X. Wang, L. Zhang, W. Hu, J. Huang, J. Yang, W. (2021). Predicting the presence and mechanism of busulfan drug-drug interactions in hematopoietic stem cell transplantation using pharmacokinetic interaction network–based molecular structure similarity and network pharmacology. European Journal of Clinical Pharmacology, 77 (4), 595–605.